Journal of
Composites Science

MDPI

Article

Optimizing DMF Utilization for Improved MXene Dispersions in Epoxy Nanocomposites

Ayyaz Ali Janjua [1], Muhammad Younas [1], Rushdan Ahmad Ilyas [2], Islam Shyha [3], Nadimul Haque Faisal [1], Fawad Inam [4,5] and Mohd Shahneel Saharudin [1,*]

[1] School of Engineering, Robert Gordon University, Aberdeen AB10 7GE, UK; a.janjua@rgu.ac.uk (A.A.J.); m.younas@rgu.ac.uk (M.Y.); n.h.faisal@rgu.ac.uk (N.H.F.)
[2] Department of Chemical Engineering, Faculty of Chemical and Energy Engineering, Universiti Teknologi Malaysia, Skudai 81310, Malaysia; ahmadilyas@utm.my
[3] School of Computing, Engineering and Built Environment, Edinburgh Napier University, 10 Colinton Road, Edinburgh EH10 5DT, UK; i.shyha@napier.ac.uk
[4] School of Architecture, Computing and Engineering, University of East London, London E16 2RD, UK; fawad.inam@oxfordbusinesscollege.ac.uk
[5] Executive Principal Office, Oxford Business College, 23-38 Hythe Bridge Street, Oxford OX1 2EP, UK
* Correspondence: s.saharudin@rgu.ac.uk; Tel.: +44-7824799021

Abstract: Dimethylformamide (DMF), a polar solvent, is commonly used for preparing graphene/epoxy nanocomposites. While previous research has commonly predominantly highlighted the improvement in physio-mechanical properties of these nanocomposites, the effect of DMF on processing and its direct influence on the final characteristics of MXene/epoxy nanocomposites have not been investigated. This unexplored link between DMF dosage, MXene concentrations, and the final composite properties presents an exciting direction for future research. In this study, a fixed dosage of DMF was used with varying MXene concentrations to fabricate the nanocomposites. To assess the reliability of DMF dosage on the characteristics of the fabricated nanocomposites, various evaluation techniques were employed, including dispersion evaluation, mechanical tests, thermogravimetric analysis (TGA), differential scanning calorimetry (DSC), scanning electron microscopy (SEM), electromagnetic interference (EMI) shielding, and surface roughness measurements. The research outcomes revealed that as MXene concentration increased, the characteristics of the MXene/epoxy nanocomposites, improved across the board, indicating their potential for use in energy storage applications.

Keywords: N,N-dimethylformamide (DMF); MXene; epoxy; nanocomposite; nanocoating; energy storage

Citation: Janjua, A.A.; Younas, M.; Ilyas, R.A.; Shyha, I.; Faisal, N.H.; Inam, F.; Saharudin, M.S. Optimizing DMF Utilization for Improved MXene Dispersions in Epoxy Nanocomposites. *J. Compos. Sci.* **2024**, *8*, 340. https://doi.org/10.3390/jcs8090340

Academic Editor: Francesco Tornabene

Received: 6 July 2024
Revised: 13 August 2024
Accepted: 28 August 2024
Published: 29 August 2024

1. Introduction

MXenes are two-dimensional nanosheets produced from transition metal carbides, nitrides, and carbonitrides which rejuvenated the current research activities in materials science. MXenes were first etched by a renowned scientist Yuri Gogotsi in 2011 from the MAX phase precursor [1–3]. MXenes have attracted significant research interest worldwide and have shown promising potential in energy storage applications [4–9], due to their layered structure, superior hydrophilicity, metallic properties, high charge-carrier mobility, tunable band gap, and rich surface chemistry [5,7]. The layered structure of MXene is joined by weak Van der Waals interactions [9–12]. MXenes possess unique electrical, optical, and mechanical attributes, which ultimately opened the new doors for researchers and scientists to conduct deep analysis in assorted fields for more than a decade [13,14]. The combination of d-block elements could possibly increase the notable MXene characteristics. However, these d-block metals possess the ability to establish an ordered layered structure in the lattice, as seen in $(Mo_{2/3}Y_{1/3})_2CT_x$, or layered atomic formations like $Mo_2TiC_2T_x$,

converting into single-layer MXene with ideal configurations. The orderly arranged MXene was first invented in 2014 and later revised the following year.

Epoxies, on the other hand, are commonly utilized in cutting-edge engineering activities because they exhibit prominent strength, low shrinkage during curing, a low level of residual stresses, and resistance to various chemicals [15–17]. Due to their molecular structure and having low viscosity, a high level of adhesion and processability can be achieved, so epoxies are regularly integrated as a matrix to impregnate the fibers during the manufacturing of fiber-reinforced plastic (FRP) composites. Researchers face challenges utilizing epoxies, due to their unfavorable characteristics [18–20]. The highly cross-linked networks result in quite low fracture toughness, which limits their use in high-end applications [21,22].

Many researchers have investigated that internal stresses are developed following curing, which reveals how a highly entangled and cross-linked polymeric chain of native epoxy leads to a low-fracture toughness. As epoxies are highly cross-linked, the crack grows without any hinderance and its advancement from the plastic deformation is constrained [10,23]. One way to improve the toughness of these brittle epoxies is by adding thermoplastics or elastomeric blends, while incorporation of nanomaterials could also promote the key properties' improvement [24,25]. In epoxy/MXene nanocomposites, MXenes can significantly improve the physical as well as chemical properties of the matrix, at minimal loadings [26,27]. However, this improvement is directly linked with the MXenes nanoparticle uniform dispersion throughout the polymeric matrix. MXenes, when they achieve uniform dispersion, can contribute to sharing the external stresses to avoid stress concentration and inhibit crack growth, resulting in improved mechanical properties [28–31]. Out of all solutions, processed MXenes, $Ti_3C_2T_x$ present the highest metallic conductivity, approaching 10,000 S/cm for films, along with a Young's modulus of 330 ± 30 GPa for a single $Ti_3C_2T_x$ flake [32–34]. These properties transform MXene into a viable candidate to use as discontinuous fibers within epoxy nanocomposites. Previous research has documented the fact that MXenes could be added as a filler material into a variety of polymers such as polyvinyl alcohol, poly-pyrrole, and sodium alginate with enhanced electrochemical properties and improved electromagnetic interference shielding (EMI) [35,36].

The research into improved properties of MXene/epoxy nanocomposites is progressing swiftly. However, in practice, the simple dispersion of MXene in epoxy polymer is not effective [37–39], as the MXene nanomaterials tend to reaggregate within a polymeric matrix due to the presence of strong Van der Waals interactions, even after homogenization [40]. A high level of dispersion of MXene within epoxy resin with relatively high viscosity is generally difficult. Therefore, using solvents as dispersion media is broadly accepted and considered as a straightforward technique to isolate the single flakes of MXene within nanocomposites.

Gogotsi investigated the dispersion of MXene in various organic solvents and concluded that N,N-dimethylformamide (DMF), N-methyl-2-pyrrolidone (NMP) and DMSO provided high-quality dispersions [1], motivated by successful dispersions of MXene in organic solvents, demonstrating potential for researching and expanding its application horizon. MXenes could possibly be blended with various nanomaterials and polymers in organic solvents to fabricate nanocomposites, which can be used for water-sensitive applications. To achieve a higher dispersion of larger MXene concentrations, two methods are reported in the literature. The solvent-exchange (SE) processing route demands various solvent transfers to gain stable dispersions of MXene in organic solvents [41]. As MXene dispersions are quite stable, the transfer of solution via the solvent-exchange method imposes restrictions. Moreover, a series of solvent exchanges are needed to lower the water content, potentially leading towards wastage of MXene solution. A substitute technique to achieve a high level of stable dispersions is the surface modification of MXene in any type of solvent. These methods involve complicated and laborious procedures, and turnaround time to explore a suitable organic solvent that could possibly stabilize the MXene disper-

sions for a longer time, with ease of processing. Therefore, there is an urgent need to develop an efficient methodology for preparing larger dispersions of MXene in organic solvents. Nevertheless, previous studies reported that the concentration of MXene stayed below 0.5 mg/mL. This showcases the current challenge of achieving a high level of MXene dispersions within organic solvents, which is mandatory for higher production. Hence, a more reliable method should be established which has the capability of achieving high MXene concentrations in organic solvents to ensure larger production while preventing agglomeration. No previous literature has investigated the effect of DMF solvent volume on the properties of MXene/epoxy nanocomposites with increasing concentrations of MXene. This research aims to study in depth the use of this solvent in the fabrication of nanocomposites.

2. Materials and Methods

Epoxy was used as the matrix material in the current research, and was fabricated utilizing EPOPHEN EL5—a bis-phenol A liquid-resin system, and EPOPHEN EHA57—a diamine catalyst, both of which were acquired from Polyfibre Ltd., Birmingham, UK. This resin system provides balanced properties, with epoxy content ranging from 4.76 to 5.25 mol/kg. EL5 is mostly liquid at room temperature, and has a viscosity of 12,000–15,000 cp, while the hardener (catalyst) is only 45 cp viscous. The mixing ratio for epoxy and hardener is 2:1, according to the guidelines from the company. This epoxy formulation was chosen because it performs quite well as a thermosetting polymeric matrix. MXenes-$Ti_3C_2T_x$, a combination of multilayer nanoflakes were procured from NanoPlexus, Manchester, UK, with the product name MXN$Ti_3C_2T_x$-FLN (Figure 1). According to the manufacturer's provided datasheet, the nanoflakes possess a surface area of 25 m^2/g, an average lateral size of 1 µm to 4 µm, and thickness of 1 nm to 3 nm. Dimethylformamide (DMF) was purchased from Sigma-Aldrich (Sigma-Aldrich Company Ltd., Gillingham, UK) with 99.9% purity.

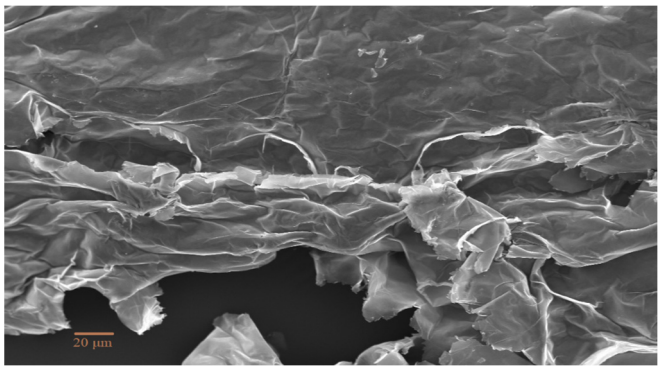

Figure 1. SEM image of MXene nanoflake.

Standard epoxy was used a reference material, and one set of samples were fabricated. Another 5 set of samples with varying MXene compositions ranging from 0.1 wt.% to 0.5 wt.% were prepared. The MXene nanoflakes were first dispersed in fixed 100 mL DMF dosage, following sonication. To understand the relationship between the quantity of DMF, nanoflake dispersion rate, and the properties of nanocomposites, 0.1 wt.% to 0.5 wt.% MXene/epoxy nanocomposites were fabricated at a fixed DMF dosage. Weighted MXene nanoflakes from 0.1 to 0.5 wt.% were first dispersed in DMF, say 100 mL, respectively, marked as D-10, D-30, D-100, D-300, and D-500, accordingly, followed by bath sonication for 60 min. Epoxy monomer was then added to the dispersion and again sonicated for another 30 min. DMF solvent was removed by heating the mixture on a hot plate while maintaining the temperature at 150 °C with constant stirring. At standard DMF dosages, the mixture was heated for 4 h to complete evaporation of the solvent. All mixtures were weighted to ensure the complete evaporation of DMF. The mixtures were cooled down to

room temperature and then the hardener was added, followed by hand stirring for two minutes. The created air bubbles were removed by placing the mixture under vacuum for a few minutes. The patterns were printed using a 3D printer, strictly following the respective ASTM standards, and these were then utilized to fabricate the rubber silicone molds. Lastly, the molds were filed with degassed mixture. Pre-curing of the nanocomposites took place at room temperature for 24 h, while the post-curing took place at 120 °C for 8 h. The nanocomposite fabrication process is shown in Figure 2.

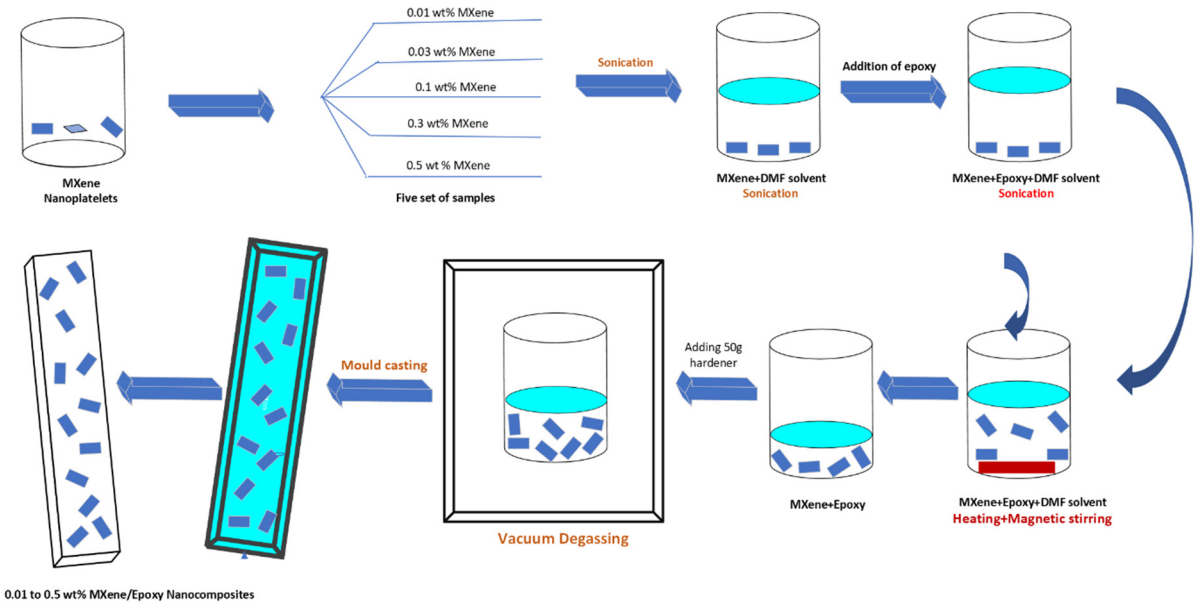

Figure 2. The schematics of nanocomposites fabrication.

A universal testing machine (Instron 3382, Instron corporation, Norwood, MA, USA) was used to conduct flexural testing, and the crosshead speed was maintained at 2 mm/min for the testing samples. Three-point flexural testing was performed following ASTM D790 with sample dimensions of 3 mm × 12.7 mm × 48 mm. The fractured surfaces of the nanocomposites were investigated using scanning electron microscopy (SEM) and analysis was conducted by the FEI Quanta 200 microscope (FEI corporation, Hillsboro, OR, USA). The fractured surfaces were cut off from the samples and a thin gold coating was applied using an Emscope sputter coater, model SC500A, (Quorum technologies Ltd., Laughton, UK). Five specimens were tested for flexural testing for each type of nanocomposites, and their mean values were reported. The nanoindentation testing of samples was performed using a Vickers hardness tester with an applied load of 2 N. Three samples of each specimen type were tested to sets and mold approximately 2 min.

Thermal properties of the nanocomposites were investigated by conducting thermogravimetric analysis (TGA) and differential scanning calorimetry (DSC) using TA Instruments Q500 thermal analyzer (TA Instruments, New Castle, DE, USA). There was a rise in temperature from room temperature to 600 °C for DSC, and from room temperature to 800 °C for the TGA analysis, with a ramp rate of 10 °C/min. The electromagnetic interference shielding (EMI) was carried out using a Multifield EMF Meter, 3.5 GHz purchased from (RS, Aberdeen, UK). It simultaneously measures the magnetic field LF with triple axis, electric field LF, and electromagnetic field RF. The surface roughness of the samples was conducted using Alicona Infinite Focus (Alicona Imaging GmbH from Raaba, Austria). It measures in 3D the dimensions, shape, and roughness with one optical sensor, with high precision and fast detection.

3. Results and Discussion

3.1. MXene Nanoflake Dispersion

A total of 10 mg MXene nanoflakes were weighed and added into 100 g of each epoxy resin, catalyst, and DMF solvent. The mixtures were sonicated using a bath sonicator, and results were compared at different parameters. For each sample, the sonication time was increased from 7 min to 60 min. One series of tests were completed at 20 °C, while the second was completed at 40 °C. The ultrasonic wave strength (amplitude) was set at 20 KHz. After finishing the sonication of samples at fixed parameters, these were poured straightaway into standard cuvettes to conduct UV-Vis spectroscopy. After sonication, spontaneous UV-Vis testing is mandatory, as the MXene nanoflakes tend to agglomerate after just a few minutes of sonication, due to strong van der Waals interactions.

3.1.1. Evaluation of UV-Light Transmittance at Fixed Temp of 20 °C

All the samples were sonicated at a fixed temperature of 20 °C, while other parameters were altered. To confirm the light transmission through each sample, UV-Vis spectroscopy was performed. Within the visible range, the wavelength of the passing light was set at 450 nm.

A huge variation in the light-transmission rate was observed in different samples (Figure 3). The standard epoxy sample exhibited a high light-transmittance rate after being sonicated for 7 min, that is, 91%. A lowering trend in the light transmittance was observed when the sonication time reached up to 60 min. The larger molecular chains of the epoxy are densely entangled, which make it very difficult for the nanoflakes to disperse easily. So, the higher sonication times reduce the resin viscosity, with increasing temperature, and results in the lowering of the light-transmittance values.

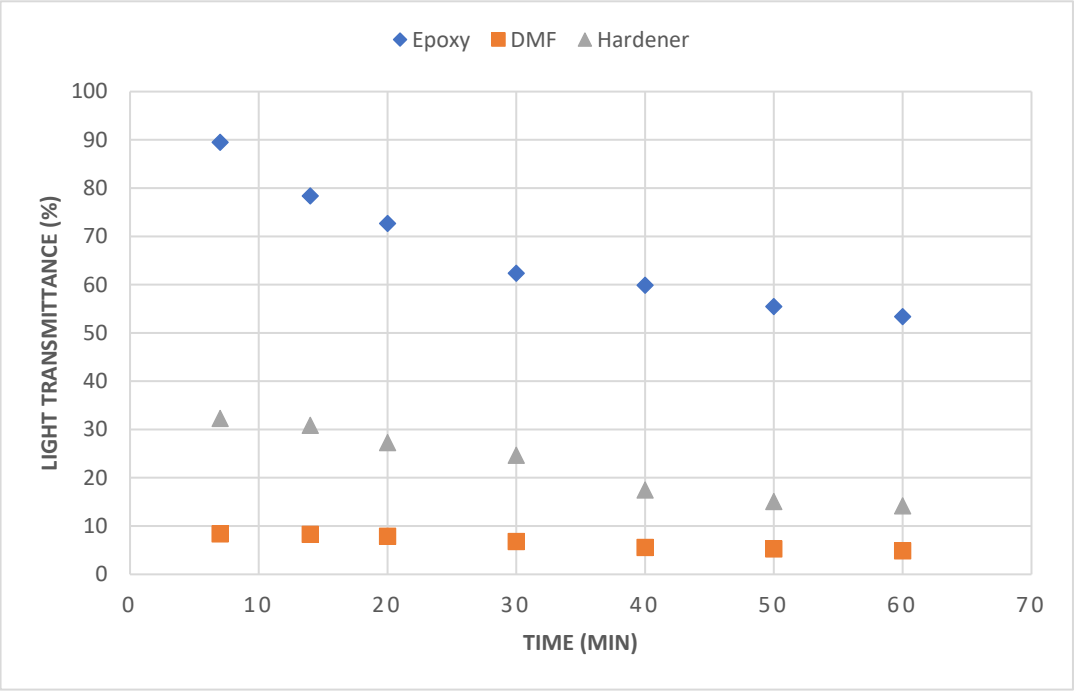

Figure 3. Shows the comparison of light transmittance through epoxy, hardener, and DMF at a fixed temperature of 20 °C.

On the other hand, compared to the epoxy, the light-transmittance behavior through the hardener (catalyst) and DMF solvent was incredible. A point to note is that a high level of dispersion state of nanoflakes was attained at lower sonication times. Both hardener and DMF have lower viscosity compared to epoxy, which helped with very low rates of light transmission. At lower sonication times, the hardener revealed a higher light-transmittance

value compared with DMF, but with increased sonication time, the transmittance declined. The results obtained from the DMF samples were quite astonishing, and their transmittance remained consistent and under 10% for 60 min. These results reveal that the DMF solvent possesses even lower viscosity compared to the hardener (catalyst).

Even though both the hardener and DMF solvent samples revealed a high level of uniform dispersion, serious issues were observed during their processing. Once the sonication is over, the nanoflakes tend to agglomerate and settle at the bottom of the flask, due to their lower viscosities, which results in a further reduction in transmittance. To tackle this issue, we performed UV–Vis spectroscopy to attain the accurate light-transmission values from these low-viscous materials.

3.1.2. Evaluation of UV-Light Transmittance at Fixed Temp of 40 °C

All the samples were sonicated at a fixed temperature of 40 °C, while their time to sonicate increased gradually, from 7 to 60 min. Light-transmission values were measured by performing UV–Vis spectroscopy. MXene nanoflakes were added separately into the epoxy, hardener, and DMF, to prepare dispersions for testing. The epoxy samples showed a drop in light transmittance from 63% to 52.6% when sonicated from 7 to 60 min (Figure 4). However, the hardener (catalyst) again revealed intermediate values. Its light-transmission values dropped from 32.3% to 14.2% when the sonication time increased from 7 to 60 min. On the other hand, DMF solvent samples again depicted extraordinary below-10% light-transmittance values at any sonication time.

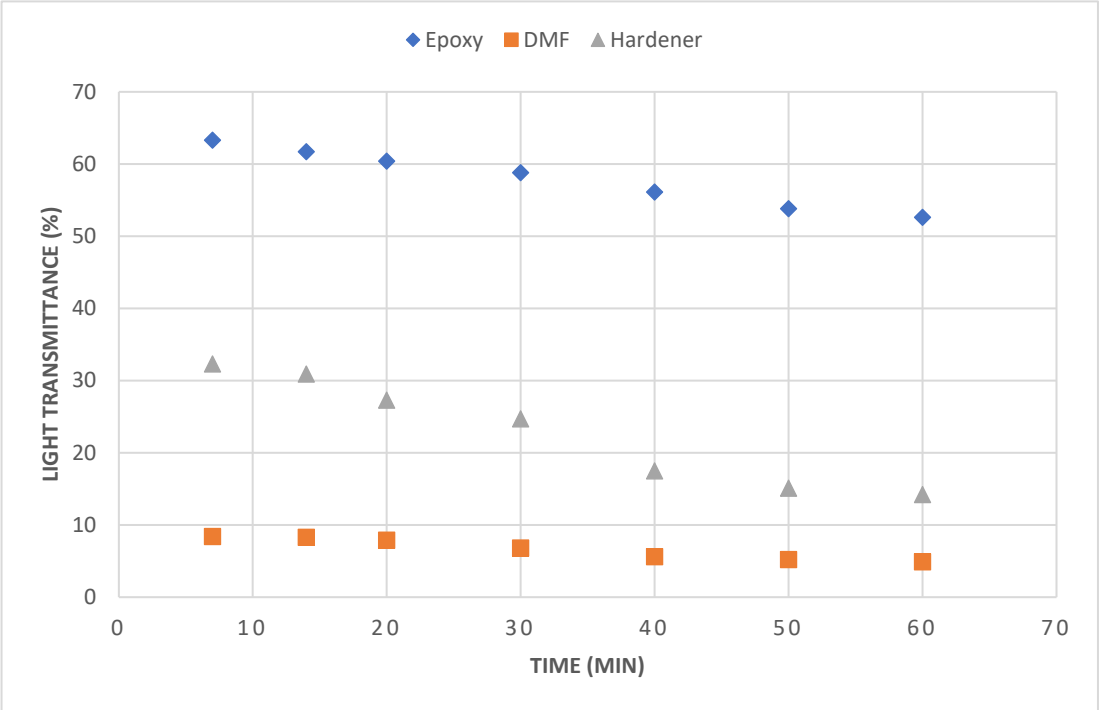

Figure 4. Showing the comparison of light transmittance through epoxy, hardener, and DMF at a fixed temperature of 40 °C.

When epoxy samples were sonicated at 20 °C for 7 min, there was a high value of light transmission, of 89.5%, while at 40 °C it dropped to 63.3%. At 40 °C, the epoxy long molecular chains were free to move, which helped the nano flakes to disperse even more uniformly, which ultimately resulted in the decline in transmission values. Again, lesser agglomerations were noticed in the samples sonicated at 40 °C, compared with 20 °C. Due to lower viscosities possessed by both the hardener and DMF, no visible change in light transmission was observed at 40 °C. The MXene nanoflakes dispersed uniformly, resulting in an absorbance rate of 1.252, which was the peak among all the experiments conducted.

3.1.3. Evaluation of UV-Light Transmittance though Epoxy

In this series of experiments, epoxy/MXene samples were sonicated at three different temperatures, that is, 20, 40, and 45 °C, along with time variation, and their light transmittance was measured using UV–vis spectroscopy. When samples were sonicated for only 7 min, at 20 °C the sample depicted a very high light transmittance of 89.5% while at 40 °C and 45 °C it dropped further, from 64.5% to 52.3% (Figure 5). However, as the sonication time was increased to 60 min, samples treated at 20 °C and 40 °C exhibited almost the same transmittance, of 52.6%, while at 45 °C it even dropped, to a very low value of 32.2%. Nevertheless, samples treated at 20 °C showed a consistent drop in light transmittance up to 30 min of sonication time, and later no appreciable drop was observed; on the contrary, at 40 °C, the transmittance went down gradually, from 64.5% to 52.6%. Interestingly, the samples treated at 45 °C depicted lower transmittance values that at any time on the graph. These results clearly state that higher temperatures trigger the lowering of the polymers' viscosity—which ultimately enhances the chain motion and helps the nanomaterials to dissipate evenly.

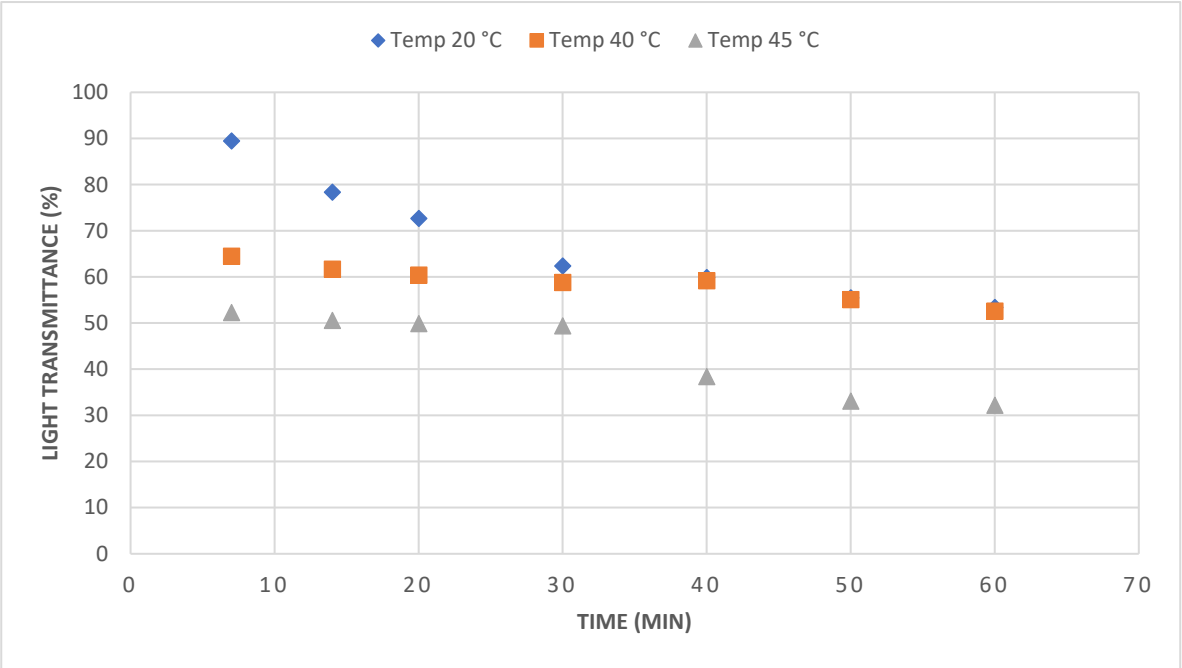

Figure 5. Shows the comparison of light transmittance through epoxy at varying temperatures.

3.1.4. Storage Life of Epoxy/MXene Dispersions

Epoxy-only/MXene samples were sonicated at 45 °C for 60 min, following the parameters set in previous findings. In the first instance, the samples were sonicated at set parameters and their UV–Vis spectroscopy was performed instantly, to investigate the light-transmission data. The samples revealed 32.4% of light transmittance after sonication (Figure 6). This value is similar with previous observations. The sample was stored for a week in a glass bottle with a lid. After a week, UV–Vis spectroscopy was again performed on the stored sample, revealing a light-transmittance value of 41.3%, which was higher compared to the sonicated sample. Similar values were found after two and four weeks. The results depict the reliability and repeatability of MXene dispersions in epoxy resin, which were stable even after weeks and months of sonication.

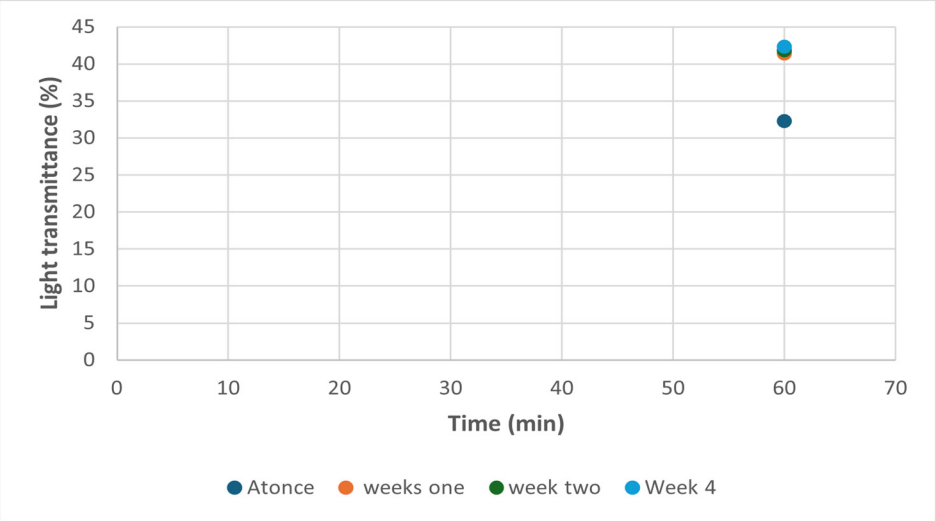

Figure 6. Showing the storage life MXene/epoxy dispersions.

3.2. Mechanical Characteristics of Nanocomposites

Previous research on MXene/epoxy nanocomposites largely focused on enhancing the mechanical attributes. However, the dispersion state of MXene nanosheets within the polymeric matrix have a significant impact on all these properties, in addition to changing the behavior of polymeric chains. The mechanical properties of the nanocomposites are summarized in Figure 7.

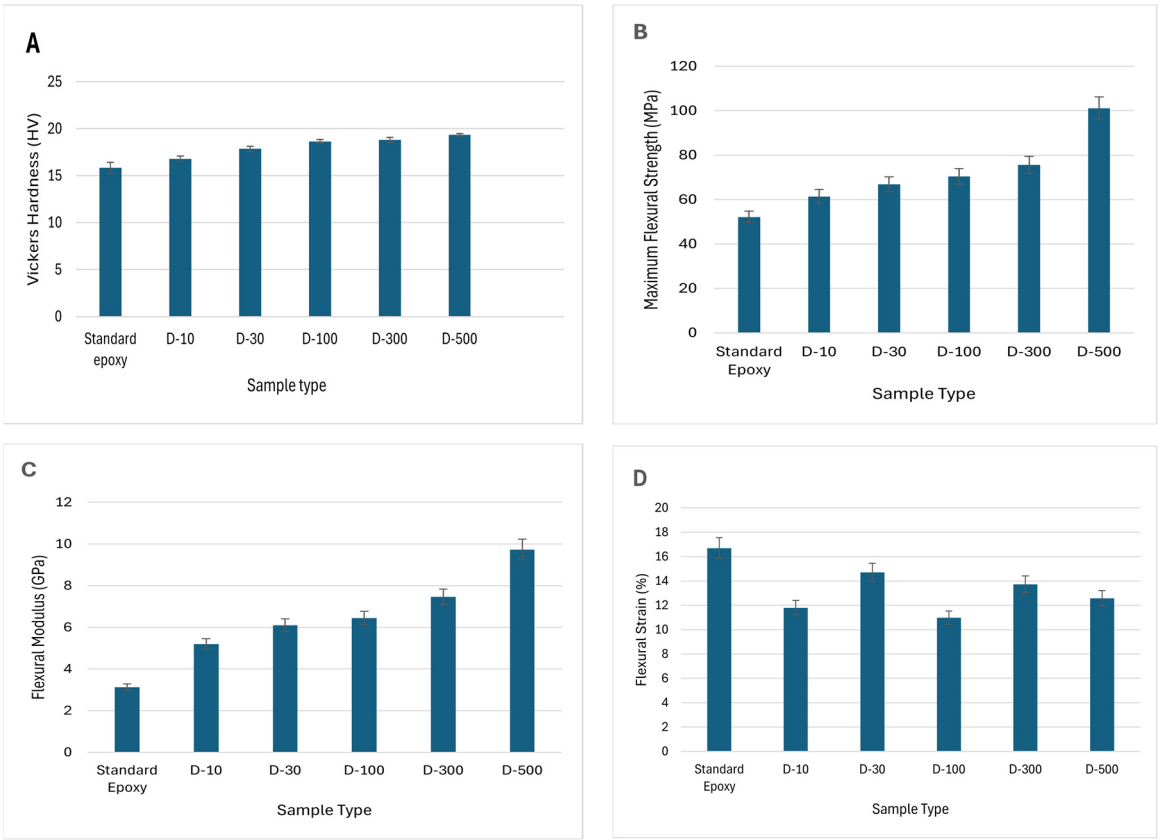

Figure 7. Mechanical properties of MXene/epoxy nanocomposites: (**A**) Vickers hardness testing; (**B**) flexural strength; (**C**) flexural modulus; and (**D**) flexural strain.

Figure 8 clearly illustrates the fact that standard epoxy samples possess the lowest mechanical attributes. Overall, the usage of DMF solvent significantly improved the mechanical properties of MXene/epoxy nanocomposites. For instance, D-500 samples showed the highest Vickers hardness values, of 19.35 HV, a high flexural strength of 100 MPa, and a flexural modulus of 9.7 GPa. the high dispersion level of MXene nanosheets within DMF played a major role. When MXene nanosheets are uniformly dispersed, it improves the materials' energy absorption and dissipation capacity, blocks the polymeric chain movement, and reduces the interface area, thereby leading to enhanced mechanical properties.

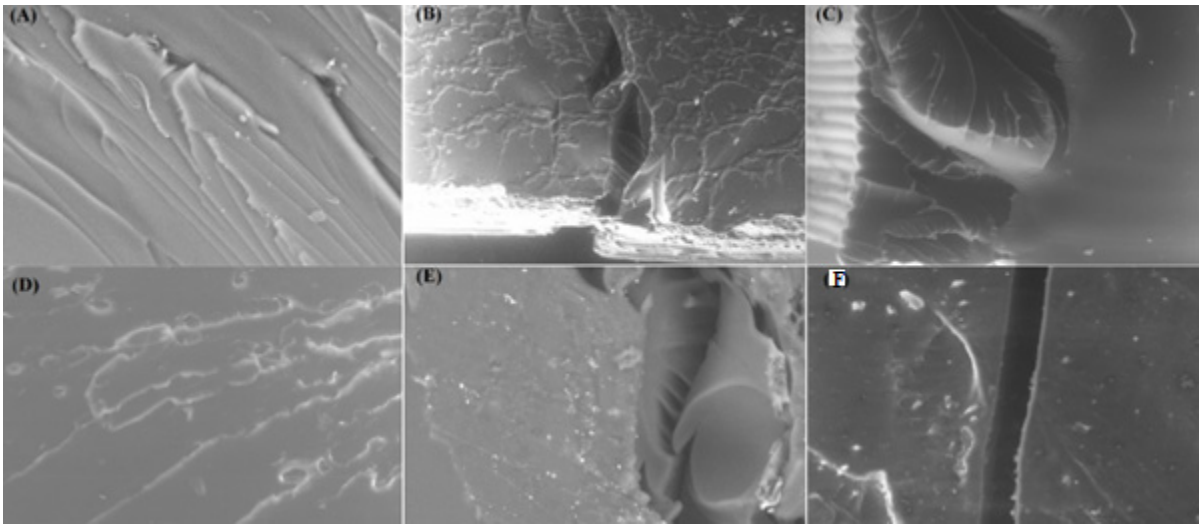

Figure 8. Flexural-test fractured surfaces under SEM: (**A**) standard epoxy, (**B**) D-10, (**C**) D-30, (**D**) D-100, (**E**) D-300, and (**F**) D-500 samples at 20 μm resolution.

On the other hand, huge variations were observed in flexural strain in different sample types. Standard epoxy samples exhibited the highest flexural-strain values, while D-100 samples showed the lowest. The highest flexural-stain values shown by the standard epoxy is due to the aging of the polymer, which resulted in plasticity, while the DMF-treated samples showed lower plasticity before rupture. This decline in flexural-strain values could be due to the re-aggregation of the MXene nanosheets which occurred during the nanocomposite manufacturing.

The morphology of the fractured surfaces is observed under the SEM microscope following flexural tests. A very smooth fracture surface can be observed in Figure 8A, indicating a brittle failure with apparent signs of plastic deformation. This depicts the epoxy-rich regions, which possibly lead towards brittle failures due to a highly crossed-linked density. For standard-epoxy samples, however, the fracture morphology took on a drastic change, from brittle to plastic deformation. Due to the aging of the standard-epoxy composite, it showed plasticity, while the rest of the nanocomposite samples showed plastic deformation before rupture. The morphological surfaces show the advancing transverse cracks which are arrested due to the presence of the MXene nanosheets. The bridging of the nanosheets can be clearly seen in the images. These images demonstrate the fact that the nanosheets are uniformly dispersed with the epoxy matrix, resulting in a strong interface area. MXene nanosheets showed their effectiveness in carrying and disseminating the external loads, which resulted in a higher mechanical strength and which can be seen in Figure 8A–E.

3.3. Thermogravimetric Analysis (TGA) of Nanocomposites

Major thermal characteristics of the nanocomposites, mandatory for different engineering applications, require their thermal decomposition at high temperatures. Interestingly, the TGA curves in Figure 9, depicted a two-stage weight-loss pattern, pointing towards a

consistent decomposition process. The first weight-loss step occurred between 50 °C and 350 °C and involved the evaporation of moisture and other thermally unstable components physically attached to the main polymer chains. The second weight-loss step occurred between 350 °C and 800 °C, where depolymerization and the breakdown of long epoxy chains are responsible for the separation of primary polymeric chains. Up to 350 °C, the epoxy showed better thermal resistance than the DMF-treated samples, while after that the DMF-treated samples absorbed more heat energy and decomposed a bit less. This variation could be due to the non-uniform dispersion of MXene flakes in these samples. The lower thermal stability of the DMF-treated samples at the start may be due to the presence of residual DMF, but with the passage of time these samples became thermally stable at higher temperatures. and decomposed less.

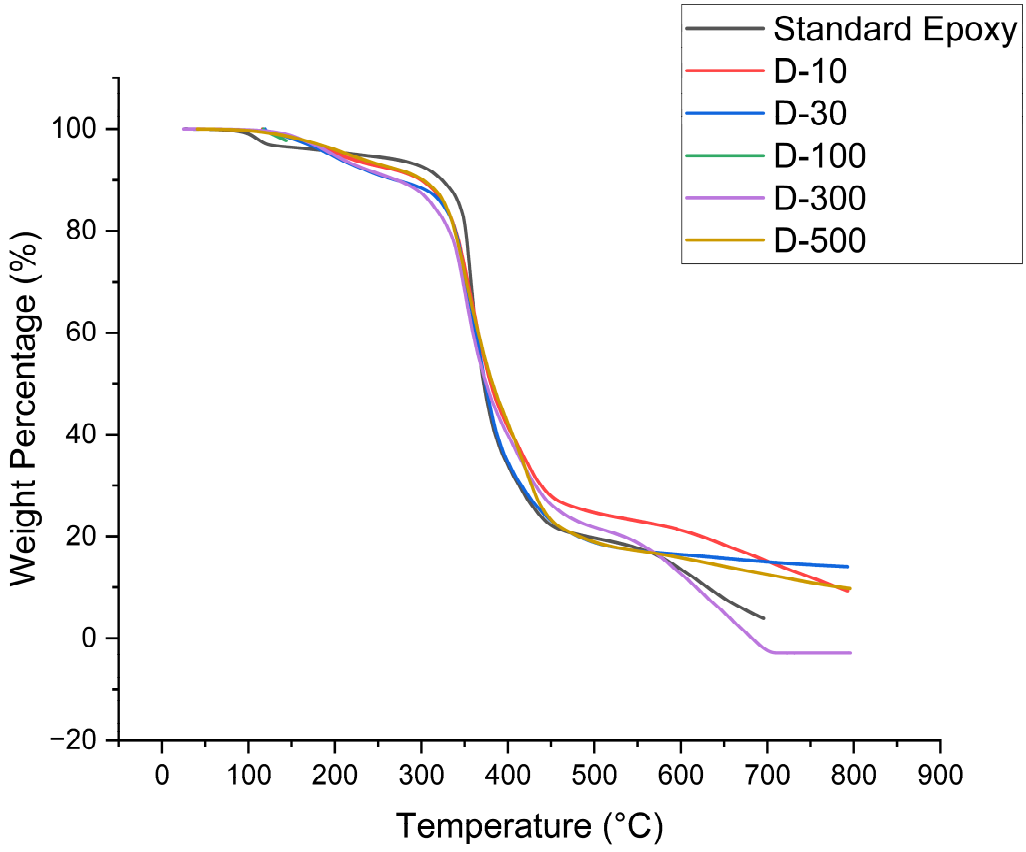

Figure 9. TGA curves of the MXene/epoxy nanocomposites.

The results revealed that the dispersion of MXene nanoplatelets has developed a strong interfacial adhesion between the polymer resin and the MXenes, effectively restricting the resin's chain movement. Remarkably, the MXene nanoplatelets within epoxy resin promote cross-linking, improving the heat stability of the densely crosslinked networks of the nanocomposites. However, this study revealed that DMF-treated MXene nanocomposites could be utilized in applications requiring a moderate temperature range, as the infusion of nanoplatelets notably improved the initial heat stability and char formation, making these nanocomposites an optimum choice for thermal management [25,28,30].

3.4. Differential Scanning Calorimetry (DSC)

The DSC curves in Figure 10 displayed endothermic peaks in the earlier test phase for all nanocomposite samples, substantiating the glass-transition (Tg) phenomenon. The standard-epoxy samples exhibited a lower Tg, of 42 °C. However, all DMF-treated nanocomposite samples depicted a higher Tg value compared to the standard epoxy. The highest Tg value of 52 °C is shown in the D-10 sample. This appreciable increase in the Tg value empha-

sizes the fact that the incorporation of MXene nanoplatelets at various weight percentages may restrict the polymeric chain motion, thus enhancing the glass-transition temperature. A region of cold crystallization can be seen in the 100 °C-to-300 °C temperature range. In this region, some of the polymer chains start melting with the temperature rise, and once they distribute heat, they become crystals again, as less heat cannot retain them in a liquid state. Nevertheless, the exothermic peaks are shown on the right-hand side of the figure, illustrating the crytallization temperature of the nanocomposite where it transitions from a disordered to an ordered state. In MXene/epoxy nanocomposites, these exothermic peaks point towards curing or cross-linking. The standard-epoxy sample possessed a crystallization temperature of 340 °C, while all DMF-treated samples exhibited a highest temperature of 350 °C, as shown by 0.5 wt.% DMF-treated MXene nanocomposite. All the DMF-treated nanocomposites exhibited an increase in crystallization temperature, due to the high level of nanoplatelet dispersion achieved. The terminal groups of the MXene made strong chemical connections with the polymeric chains, while their tunneling effect helped in the dissipation of heat, resulting in an improved crystallization temperature. Also, this increase in the crystallization temperature demonstrated the fact that nanoplatelets might behave as nucleating agents, which could promote a perfect crystalline ordered arrangement during curing.

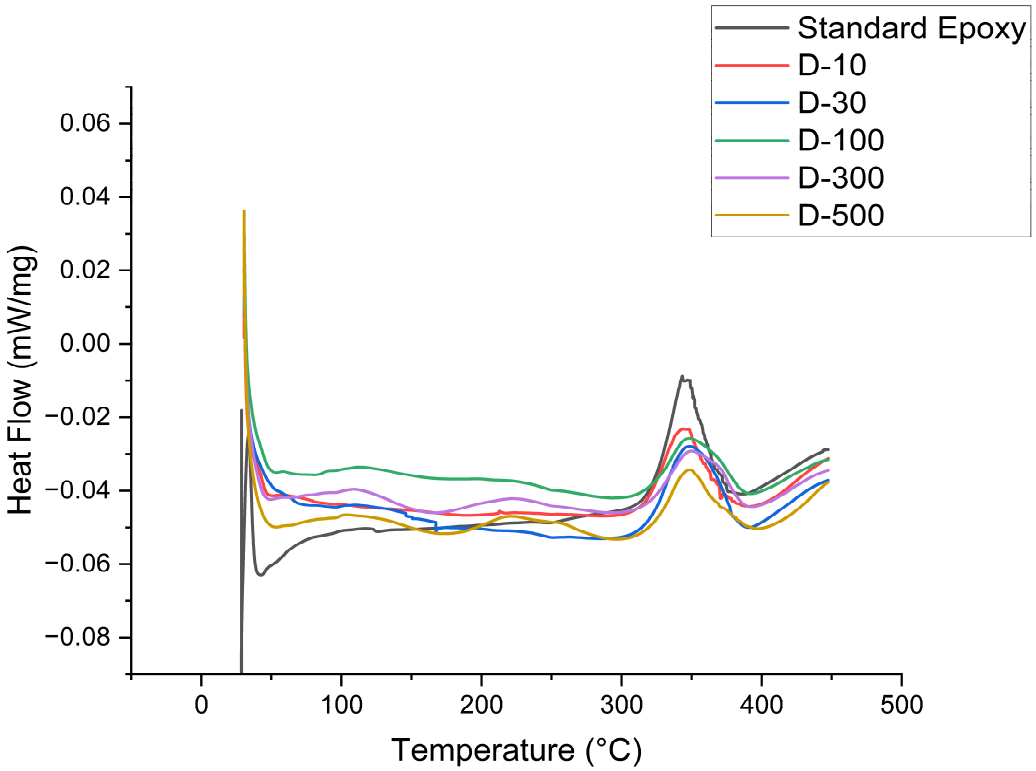

Figure 10. DSC curves of MXene/epoxy nanocomposites.

3.5. EMI Shielding of MXene/Epoxy Nanocomposites

To protect the electronic devices and humans from the effect of electromagnetic radiation, EMI shielding is a key phenomenon. The most important property possessed by EMI shielding materials is their high metallic conductivity. The minimum conductivity value required by the EMI shielding materials is 1 S/cm; however, different MXene compositions have a conductivity in the range of 5 S/cm to 20,000 S/cm. The high electric conductivity of MXenes places them among the top suitable EMI-shielding materials [3,37]. MXene films are composed of layered two-dimensional MXene sheets, which drastically enhances the electrical conductivity. Their innovative design features differentiate them from conventional EMI-shielding materials but also involves the absorption of incoming

electromagnetic waves. The integration of a conductive filler in conductive polymeric composites (CPCs) is generally considered as a new generation of materials for EMI shielding, because they are lightweight, corrosion-resistant, and have easy processability.

Six types of nanocoatings were prepared at varying MXene concentrations, including standard epoxy as a reference. EF80 flexible epoxy resin and EF80 hardener were utilized in the fabrication of nanocoatings, both procured from Easy Composites, UK. Firstly, preweighted MXene nanosheets were added to flexible epoxy resin, followed by sonication for the disintegration and uniform dispersion of the MXene sheets. The resin-to-hardener ratio was 100:145. Then the hardener was added, and the mixture was manually stirred for 2 min and put under vacuum to remove any entrapped air bubbles. Polyester peel ply fabric was coated with the mixture, following dip coating. The fabric was completely soaked in solution, allowing the formation of uniform nanocoating's. After five minutes, the cloth was removed at slow speed, so that the coating remained uniform across the cloth. The pre-curing took place at room temperature for 24 h, followed by post-curing at 120 C for 6 h. The purpose of utilizing flexible epoxy resin is that it behaves plastically and was able to completely cover the mobile phone with two-to-three wraps for subsequent EMI-shielding test.

The coatings were wrapped around a cellular phone and their EMI properties were investigated using a Seeit Multifield EMF meter, 3.5 GHz. Figure 11A illustrates the fact that the magnetic field properties of the nanocoating declines with the increasing concentration of MXene nanosheets. Likewise, Figure 11B shows results for the electric field with the same declining trend. The lowest magnetic- and electric-field values are shown for the 0.5 wt.% MXene nanocoating. This downtrend clearly states that the nanosheets were uniformly dispersed and helped in absorbing more radiation. These findings suggest that an increase in MXene concentration will render these values as zero.

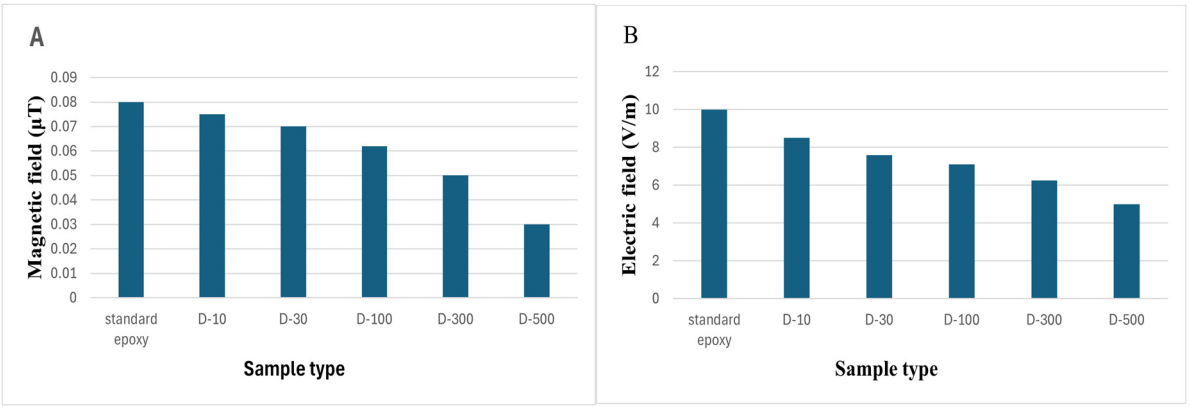

Figure 11. (**A**) magnetic-field properties and (**B**) electric-field properties.

3.6. Surface Roughness Tests

The surface roughness tests of the fractured nanocomposite surfaces were performed using Alicona Infinite Focus. Figure 12 illustrates the Ra, Rq, and Rz values, which describe the surface texture in different ways. Ra (arithmetic mean roughness) provides the average surface roughness, which gives a general idea of the surface texture. However, it does not distinguish between peaks and valleys; it only provides an average of all deviations. Rq (root mean square roughness) emphasizes the larger deviations and is slightly higher than Ra in most cases. It is more sensitive to larger peaks or valleys on the surface. Rz (maximum height of the profile) measures the height difference between peaks and valleys, providing insight into extremes of surface roughness. Ra, Rq, and Rz values of different sample types indicate that, with increasing MXene concentration, these values gradually fall off. A decline in the roughness parameters at higher MXene concentrations reveals that nanosheets are well dispersed and create strong chemical interactions with the polymeric matrix.

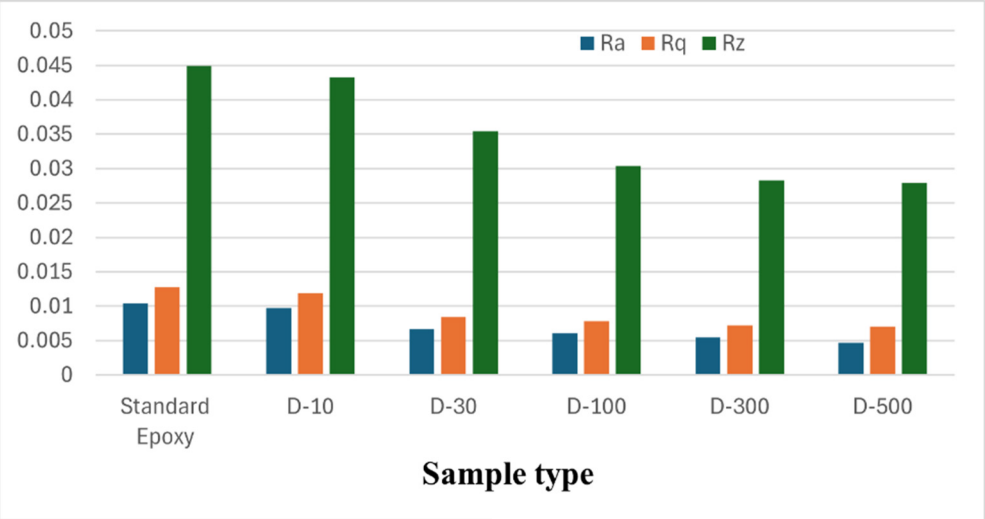

Figure 12. Ra—average roughness, Rq—root mean square roughness, and Rz—maximum height of the profile.

The Rq values are a bit higher than the Ra values for the same surface, as Rq values are more sensitive to peaks and valleys. While Rz indicates the maximum peak-to-valley height, it provides in-depth information about the outer-surface features. All declining values indicate that the surfaces are becoming less rough, but some important features still persist.

However, increasing the MXene nanosheet concentration improved the mechanical, thermal, and EMI-shielding properties; the 0.5 wt.% MXene concentration performed exceptionally well in enhancing different properties of the nanocomposite. This suggests that the terminal groups present on the MXene nanosheets established a favorable structure–property relationship with the epoxy matrix.

4. Discussion

The two-dimensional MXenes have the potential to emerge as ideal materials for fabricating the next generation of energy storage devices, because they possess a unique atomic and layered structure. The MXene nanosheets are ideal candidates for energy storage devices such as supercapacitors and different type of batteries, due to their higher surface area, high electrical conduction, and quick ion-diffusion rates. Supercapacitors represent one of the most thrilling applications of MXene nanosheets in energy storage devices. These devices can charge and discharge quickly, and are perfect for use in high-end power applications. Owing to their large surface area at the nanoscale and high conductivity, MXenes have shown high capacitance and quick charge and discharge cycles. Moreover, the terminal groups of MXenes can be tailored to improve their electrochemical performance by increasing their specific capacitance or decline in impedance. MXene could also be used in the manufacturing of energy storage batteries. These nanomaterials might be used as anodes, cathodes, or both, in Li-ion or Na-ion batteries. These are the ideal candidates for future energy-storage applications as they have high specific capacities, enhanced cycling stability, and quick charge/discharge cycles. The unique attributes associated with MXenes, including their higher surface area, enhanced metallic conduction, and very fast diffusion rates, due to the tunneling effect, document them as ideal materials in energy storage devices. Further research and development in energy storage applications is mandatory, including supercapacitors and various batteries being seen as a promising use. These MXenes could also be utilized in the fabrication of type-4 composite pressure vessels for hydrogen storage. Type-4 pressure vessels have a polymer liner, inside which there is no capability of stopping the leakage of hydrogen gas, owing to its small size. The integration of MXene in these polymer liners provides two-way benefits, in terms of

mechanical integrity as well as their small size, as they possess a larger surface area, which would aid in stopping the leakage.

5. Conclusions

In this research, DMF, a polar solvent, was used to study the effects on the dispersion of MXenes, and the formation and different characteristics of Mxene/epoxy nanocomposites. This comprehensive study provides enough details about the introduction of DMF solvent for reducing the Van der Waals interaction between MXene nanosheets and their uniform dispersion, and could also be used as a reference for the dispersion of various type of nanomaterials. In this study, MXene dispersion level, mechanical properties, SEM analysis, TGA, DSC, EMI shielding effectiveness, and surface roughness were analyzed. All the results demonstrated that increasing the concentration of MXene enhanced the properties of the nanocomposites. The usage of DMF helped in overcoming the strong Van der Waals interactions between the MXene nanosheets, and dispersed them uniformly, but they possess long processing times and higher temperatures. No noticeable agglomeration of nanosheets was found, even when 0.5 wt.% of MXene was added. This uniform dispersion of nanosheets accounts for the improved properties of MXene/epoxy nanocomposites. For a small concentration of nanosheets, we could reduce the processing time by utilizing a lower volume of solvents, thus benefiting both economically and from a health perspective. These results would aid in the optimization of processing parameters for nanocomposite fabrication. However, this research documented the relationship between the solvent dosage, MXene concentration, and processing of MXene/epoxy nanocomposites for the first time, and it has identified the optimum dispersion parameters in various media. Therefore, further study is required to better understand the solvent behavior at higher concentrations of MXene.

Author Contributions: Conceptualization, M.S.S., M.Y., F.I., N.H.F. and A.A.J.; methodology, M.S.S. and M.Y.; validation, F.I., A.A.J. and R.A.I.; formal analysis, A.A.J.; investigation, A.A.J. and M.S.S.; resources, I.S. and M.S.S.; data curation, A.A.J.; writing—original draft preparation, A.A.J.; writing—review and editing, I.S. and N.H.F.; visualization, A.A.J.; supervision, M.S.S.; project administration, M.S.S.; funding acquisition, M.S.S. and N.H.F. All authors have read and agreed to the published version of the manuscript.

Funding: This research was funded by a grant from the Carnegie Trust for the Universities of Scotland (Grant No. 1769240).

Data Availability Statement: The data presented in this study are openly available upon request. [University website] [https://rgu-research.worktribe.com/record.jx?recordid=1769240].

Acknowledgments: We would like to thank the Carnegie Trust (Project ID 1769240) for the research funding and Edinburgh Napier University for providing the Alicona Infinite Focus equipment for surface roughness measurement; without their contributions, this research would not have been possible.

Conflicts of Interest: The authors declare no conflicts of interest.

References

1. Naguib, M.; Barsoum, M.W.; Gogotsi, Y. Ten Years of Progress in the Synthesis and Development of MXenes. *Adv. Mater.* **2021**, *33*, 2103393. [CrossRef]
2. Hatter, C.B.; Shah, J.; Anasori, B.; Gogotsi, Y. Micromechanical Response of Two-Dimensional Transition Metal Carbonitride (MXene) Reinforced Epoxy Composites. *Compos. B Eng.* **2020**, *182*, 107603. [CrossRef]
3. Iqbal, A.; Sambyal, P.; Kwon, J.; Han, M.; Hong, J.; Kim, S.J.; Kim, M.K.; Gogotsi, Y.; Koo, C.M. Enhanced Absorption of Electromagnetic Waves in Ti3C2Tx MXene Films with Segregated Polymer Inclusions. *Compos. Sci. Technol.* **2021**, *213*, 108878. [CrossRef]
4. Lin, L.; Ning, H.; Song, S.; Xu, C.; Hu, N. Flexible Electrochemical Energy Storage: The Role of Composite Materials. *Compos. Sci. Technol.* **2020**, *192*, 108102. [CrossRef]
5. Jamil, F.; Ali, H.M.; Janjua, M.M. MXene Based Advanced Materials for Thermal Energy Storage: A Recent Review. *J. Energy Storage* **2021**, *35*, 102322. [CrossRef]

6. Liu, C.; Li, F.; Lai-Peng, M.; Cheng, H.M. Advanced Materials for Energy Storage. *Adv. Mater.* **2010**, *22*, E28–E62. [CrossRef]
7. Ezika, A.C.; Sadiku, E.R.; Idumah, C.I.; Ray, S.S.; Hamam, Y. On Energy Storage Capacity of Conductive MXene Hybrid Nanoarchitectures. *J. Energy Storage* **2022**, *45*, 103686. [CrossRef]
8. Zhou, Y.; Wang, Q. Ferroelectric Polymer Composites for Capacitive Energy Storage. In *Organic Ferroelectric Materials and Applications*; Elsevier: Amsterdam, The Netherlands, 2022; pp. 477–502.
9. Liu, Y.; Yu, J.; Guo, D.; Li, Z.; Su, Y. Ti3C2Tx MXene/Graphene Nanocomposites: Synthesis and Application in Electrochemical Energy Storage. *J. Alloys Compd.* **2020**, *815*, 152403. [CrossRef]
10. Wei, J.; Saharudin, M.S.; Vo, T.; Inam, F. N,N-Dimethylformamide (DMF) Usage in Epoxy/Graphene Nanocomposites: Problems Associated with Reaggregation. *Polymers* **2017**, *9*, 193. [CrossRef]
11. Riazi, H.; Nemani, S.K.; Grady, M.C.; Anasori, B.; Soroush, M. Ti3C2MXene-Polymer Nanocomposites and Their Applications. *J. Mater. Chem. A Mater.* **2021**, *9*, 8051–8098. [CrossRef]
12. Saharudin, M.S.; Ilyas, R.A.; Awang, N.; Hasbi, S.; Shyha, I.; Inam, F. Advances in Sustainable Nanocomposites. *Sustainability* **2023**, *15*, 5125. [CrossRef]
13. Tang, T.; Wang, S.; Jiang, Y.; Xu, Z.; Chen, Y.; Peng, T.; Khan, F.; Feng, J.; Song, P.; Zhao, Y. Flexible and Flame-Retarding Phosphorylated MXene/Polypropylene Composites for Efficient Electromagnetic Interference Shielding. *J. Mater. Sci. Technol.* **2022**, *111*, 66–75. [CrossRef]
14. Che Nasir, N.A.; Saharudin, M.S.; Wan Jusoh, W.N.; Kooi, O.S. Effect of Nanofillers on the Mechanical Properties of Epoxy Nanocomposites. In *Advanced Structured Materials*; Springer: Cham, Switzerland, 2022; Volume 167.
15. Saharudin, M.S.; Atif, R.; Shyha, I.; Inam, F. The Degradation of Mechanical Properties in Polymer Nano-Composites Exposed to Liquid Media—A Review. *RSC Adv.* **2016**, *6*, 1076–1089. [CrossRef]
16. Wei, J.; Saharudin, M.S.; Vo, T.; Inam, F. Effects of Surfactants on the Properties of Epoxy/Graphene Nanocomposites. *J. Reinf. Plast. Compos.* **2018**, *37*, 960–967. [CrossRef]
17. Wazalwar, R.; Tripathi, M.; Raichur, A.M. Curing Behavior and Mechanical Properties of Tetra-Functional Epoxy Reinforced with Polyethyleneimine-Functionalized MXene. *ACS Appl. Polym. Mater.* **2022**, *4*, 2573–2584. [CrossRef]
18. Bukichev, Y.S.; Bogdanova, L.M.; Lesnichaya, V.A.; Chukanov, N.V.; Golubeva, N.D.; Dzhardimalieva, G.I. Mechanical and Thermophysical Properties of Epoxy Nanocomposites with Titanium Dioxide Nanoparticles. *Appl. Sci.* **2023**, *13*, 4488. [CrossRef]
19. Dong, M.; Zhang, H.; Tzounis, L.; Santagiuliana, G.; Bilotti, E.; Papageorgiou, D.G. Multifunctional Epoxy Nanocomposites Reinforced by Two-Dimensional Materials: A Review. *Carbon* **2021**, *185*, 57–81. [CrossRef]
20. Chen, J.; Wang, S.; Du, X. Advances in Epoxy/Two-Dimensional Nanomaterial Composites. *Cailiao Daobao/Mater. Rep.* **2021**, *35*, 17210–17217.
21. Sliozberg, Y.; Andzelm, J.; Hatter, C.B.; Anasori, B.; Gogotsi, Y.; Hall, A. Interface Binding and Mechanical Properties of MXene-Epoxy Nanocomposites. *Compos. Sci. Technol.* **2020**, *192*, 108124. [CrossRef]
22. Zukiene, K.; Monastyreckis, G.; Kilikevicius, S.; Procházka, M.; Micusik, M.; Omastová, M.; Aniskevich, A.; Zeleniakiene, D. Wettability of MXene and Its Interfacial Adhesion with Epoxy Resin. *Mater. Chem. Phys.* **2021**, *257*, 123820. [CrossRef]
23. Li, C.; Xu, J.; Xu, Q.; Xue, G.; Yu, H.; Wang, X.; Lu, J.; Cui, G.; Gu, G. Synthesis of Ti3C2 MXene@PANI Composites for Excellent Anticorrosion Performance of Waterborne Epoxy Coating. *Prog. Org. Coat.* **2022**, *165*, 106673. [CrossRef]
24. Saharudin, M.S.; Wei, J.; Shyha, I.; Inam, F. Biodegradation of Halloysite Nanotubes-Polyester Nanocomposites Exposed to Short Term Seawater Immersion. *Polymers* **2017**, *9*, 314. [CrossRef] [PubMed]
25. Giménez, R.; Serrano, B.; San-Miguel, V.; Cabanelas, J.C. Recent Advances in MXene/Epoxy Composites: Trends and Prospects. *Polymers* **2022**, *14*, 1170. [CrossRef]
26. Lee, S.; Kim, J. Incorporating MXene into Boron Nitride/Poly(Vinyl Alcohol) Composite Films to Enhance Thermal Andmechanical Properties. *Polymers* **2021**, *13*, 379. [CrossRef]
27. Qian, Y.; Zhong, J.; Ou, J. Superdurable Fiber-Reinforced Composite Enabled by Synergistic Bridging Effects of MXene and Carbon Nanotubes. *Carbon* **2022**, *190*, 104–114. [CrossRef]
28. Ding, R.; Sun, Y.; Lee, J.; Nam, J.D.; Suhr, J. Enhancing Interfacial Properties of Carbon Fiber Reinforced Epoxy Composites by Grafting MXene Sheets (Ti2C). *Compos. B Eng.* **2021**, *207*, 108580. [CrossRef]
29. Feng, A.; Hou, T.; Jia, Z.; Zhang, Y.; Zhang, F.; Wu, G. Preparation and Characterization of Epoxy Resin Filled with Ti3C2Tx MXene Nanosheets with Excellent Electric Conductivity. *Nanomaterials* **2020**, *10*, 108580. [CrossRef] [PubMed]
30. Zhu, Q.; Li, J.; Simon, P.; Xu, B. Two-Dimensional MXenes for Electrochemical Capacitor Applications: Progress, Challenges and Perspectives. *Energy Storage Mater.* **2021**, *35*, 630–660. [CrossRef]
31. Iqbal, A.; Hong, J.; Ko, T.Y.; Koo, C.M. Improving Oxidation Stability of 2D MXenes: Synthesis, Storage Media, and Conditions. *Nano Converg.* **2021**, *8*, 9. [CrossRef]
32. Xie, F.; Jia, F.; Zhuo, L.; Lu, Z.; Si, L.; Huang, J.; Zhang, M.; Ma, Q. Ultrathin MXene/Aramid Nanofiber Composite Paper with Excellent Mechanical Properties for Efficient Electromagnetic Interference Shielding. *Nanoscale* **2019**, *11*, 23382–23391. [CrossRef]
33. Wang, Z.; Cheng, Z.; Fang, C.; Hou, X.; Xie, L. Recent Advances in MXenes Composites for Electromagnetic Interference Shielding and Microwave Absorption. *Compos. Part. A Appl. Sci. Manuf.* **2020**, *136*, 105956. [CrossRef]
34. Wang, L.; Chen, L.; Song, P.; Liang, C.; Lu, Y.; Qiu, H.; Zhang, Y.; Kong, J.; Gu, J. Fabrication on the Annealed Ti3C2Tx MXene/Epoxy Nanocomposites for Electromagnetic Interference Shielding Application. *Compos. B Eng.* **2019**, *171*, 111–118. [CrossRef]

35. Gong, K.; Zhou, K.; Qian, X.; Shi, C.; Yu, B. MXene as Emerging Nanofillers for High-Performance Polymer Composites: A Review. *Compos. B Eng.* **2021**, *217*, 108867. [CrossRef]
36. Wei, J.; Vo, T.; Inam, F. Epoxy/Graphene Nanocomposites—Processing and Properties: A Review. *RSC Adv.* **2015**, *5*, 73510–73524. [CrossRef]
37. Wei, J.; Atif, R.; Vo, T.; Inam, F. Graphene Nanoplatelets in Epoxy System: Dispersion, Reaggregation, and Mechanical Properties of Nanocomposites. *J. Nanomater.* **2015**, *2015*, 561742. [CrossRef]
38. Ronchi, R.M.; Arantes, J.T.; Santos, S.F. Synthesis, Structure, Properties and Applications of MXenes: Current Status and Perspectives. *Ceram. Int.* **2019**, *45*, 18167–18188. [CrossRef]
39. Wei, J.; Saharudin, M.S.; Vo, T.; Inam, F. Dichlorobenzene: An Effective Solvent for Epoxy/Graphene Nanocomposites Preparation. *R. Soc. Open Sci.* **2017**, *4*, 170778. [CrossRef]
40. Yu, B.; Yuen, A.C.Y.; Xu, X.; Zhang, Z.C.; Yang, W.; Lu, H.; Fei, B.; Yeoh, G.H.; Song, P.; Wang, H. Engineering MXene Surface with POSS for Reducing Fire Hazards of Polystyrene with Enhanced Thermal Stability. *J. Hazard. Mater.* **2021**, *401*, 123342. [CrossRef] [PubMed]
41. Jimmy, J.; Kandasubramanian, B. Mxene Functionalized Polymer Composites: Synthesis and Applications. *Eur. Polym. J.* **2020**, *122*, 109367. [CrossRef]